J. Soil Groundw. Environ. Vol. 20(2), p. 41~46, 2015
http://dx.doi.org/10.7857/JSGE.2015.20.2.041
≪ **Research Paper** ≫
ISSN 1598-6438 (Print), ISSN 2287-8831 (Online)

Feasibility of Streaming Potential Signal on Estimation of Solute Transport Characteristics

Mohammad Lutful Kabir[1,2] · Sung- Hoon Ji[1]* · Jin-Yong Lee[2] · Yong- Kwon Koh[1]

[1]*Radioactive Waste Disposal Research Division, Korea Atomic Energy Research Institute*

[2]*Department of Geology, Kangwon National University*

ABSTRACT

The drag of the excess charge in an electrical double layer at the solid fluid interface due to water flow induces the streaming current, i.e., the streaming potential (SP). Here we introduce a sandbox experiment to study this hydroelectric coupling in case of a tracer test. An acrylic tank was filled up with homogeneous sand as a sand aquifer, and the upstream and downstream reservoirs were connected to the sand aquifer to control the hydraulic gradient. Under a steady-state water flow condition, a tracer test was performed in the sandbox with the help of peristaltic pump, and tracer samples were collected from the same interval of five screened wells in the sandbox. During the tracer test, SP signals resulting from the distribution of 20 nonpolarizable electrodes were measured at the top of the tank by a multichannel meter. The results showed that there were changes in the observed SP after injection of tracer, which indicated that the SP was likely to be related to the solute transport.

Key words : Streaming potential (SP), Solute transport, Tracer test, Sandbox

1. Introduction

Generally, fluid flow in a porous medium and then the drag of excess charge in an electrical double layer at solid-fluid interface introduce a streaming current, and the associated electrical potential is a streaming potential (SP) (Lorne et al., 1999). The SP measurement is one of the oldest methods in geophysical techniques. It consists of monitoring electrical field existing at the ground surface of the earth where the SP signals provide the evidence of polarization mechanisms existing in the grounds. The use of the SP in different aspect of geology has been developed for the last two decades and these methods have been used for a variety of geophysical applications to detect and monitor water flow (e.g., Blake and Clarke, 1999) and leakage zones of dam (e.g., Bogoslovsky and Ogilvy, 1970; Titov et al., 2000). The SP was also used to detect the ore bodies and contaminant plumes that are rich in organic matter associated with the electro redox effect (e.g., Arora et al., 2007; Jardani et al., 2008). Because the SP is directly occurred by the hydraulic gradients in porous media and is very sensitive to the actual water, however, the major contribution of SP has been to characterize fully or partially saturated media (e.g., Fournier, 1989; Mikhailov et al., 1997; Doussan et al., 2002; Suski et al., 2004; Revil et al., 2004; Saunders et al., 2008).

During a hydraulic test, which is the classical method used to obtain information about the distribution of hydraulic properties of an aquifer, SP signals can be recorded at the ground surface by measuring electric potential differences between the nonpolarized electrodes by voltmeter and these electrodes are usually set up with the direction of water flow. Groundwater flows through a porous medium, and SP is changed due to excess charge of the pore water at the nearby mineral-pore water interface. The change of SP helps for detecting the fluid flow to characterize the hydraulic properties of the medium. Rizzo et al. (2004) estimated the hydraulic properties of an aquifer from hydraulic head and SP signals through numerical modeling with associated hydraulic tests. Malama et al. (2009a, 2009b) developed

*Corresponding author : shji@kaeri.re.kr
Received : 2015. 3. 29 Reviewed : 2015. 4. 25 Accepted : 2015. 4. 25
Discussion until : 2015. 6. 30

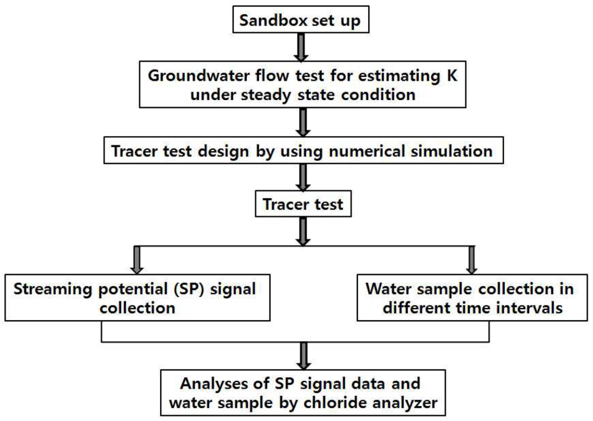

Fig. 1. Flow chart of this study.

semi-analytical solution for transient streaming potentials associated with axial symmetric flow by pumping in the confined and unconfined aquifers.

Here we present a sandbox experiment to check the feasibility of SP to estimate solute transport characteristics of an aquifer. We conducted tracer tests under steady-state groundwater flow condition with recording SP signals. We used an acrylic tank filled with medium to coarse grained sand and infiltrated with water, and tried to detect the changes in SP signals due to injection and transport of tracer.

2. Materials and Methods

Fig. 1 is the flow chart of this study. An acrylic tank was prepared for the experiment, and filled with homogeneous sand which was medium to coarse grained quartz sand with clay particles. Two reservoirs were connected to the sandbox, and they were upstream and downstream reservoirs which were used to control the water flow condition in the sandbox by overflowing water from the pipe connected to the bottom of the two reservoirs. The total length of the acrylic tank was 2.5 m with the sandbox of 1.5 m, the upstream reservoir of 0.5 m and the downstream reservoir of 0.5 m, and its height was 1.0 m as shown in Fig. 2. The upstream and downstream reservoirs were separated from the sandbox by 200 μm stainless steel mesh. Here we used five plastic screened wells which were around 1.5 cm in diameter and 1.0 m long. These screened wells included micro holes with the diameter of 0.2 cm to infiltrate water and were covered by 200 μm plastic mesh not to fill with

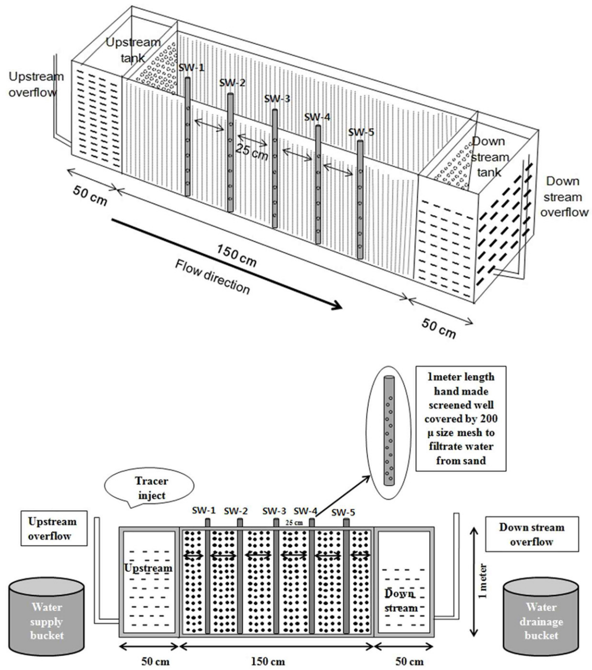

Fig. 2. Design of the sandbox.

sand during the experiments and to collect water sample uninterruptedly (Fig. 2). The screened wells set parallel at the middle of the sandbox about 25 cm distances each other. The tops of the wells were open in the air, and bottoms were sealed into the sandbox. 20 sintered Ag/AgCl nonpolarizing electrodes were installed at the top of the sand aquifer, and they surrounded the screened wells with definite distance of 8 cm to collect SP signals in the sandbox during the experiments (Crespy et al., 2008; Martinez-Pagan et al., 2010). Fig. 3 shows the setting of the instrument for the experiment.

The hydraulic conductivity of the sandbox was determined through groundwater flow tests. For the tests, the steady-state condition of groundwater flow was established by maintaining the hydraulic head difference between the upstream and downstream reservoirs. After establishing the steady-state condition, we measured the out-flow rate at the downstream of the sandbox and calculated the hydraulic conductivity using equation (1) which was from Darcy's law:

$$K = \frac{q}{Ai} \quad (1)$$

where q is the out-flow rate [m^3/sec], A is the cross sec-

Fig. 3. Full set up of a sandbox experiment.

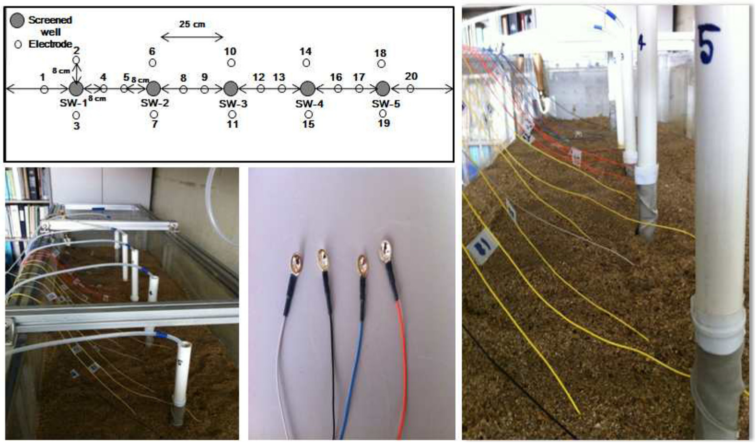

Fig. 4. Electrode set up into the sandbox.

tional area of the sandbox [m^2], L is the length of the sandbox [m], H is the hydraulic head [m], and i is the hydraulic gradient given by $i = \frac{H_{upstream} - H_{downstream}}{L}$. In this study, we estimated the hydraulic conductivity with several hydraulic head differences. Using the estimated hydraulic conductivity, we simulated the tracer test for its design. From the simulation we determined the optimal injection rate and sampling intervals. In the simulation, we assumed the effective porosity and longitudinal dispersivity to 0.15 and 0.1 m, respectively, referring to Domenico and Schwartz (1990).

A tracer test was also conducted using the sandbox. NaCl solution with the concentration of 1000 ppm was used as a tracer. We injected the tracer into the second screened well for five minutes. Before and after tracer injection, water was injected to the injection well with the same injection rate to maintain the water flow condition during the whole experiment. We collected water samples from each of the five screened wells using disposable syringes, and analyzed their concentration with the chloride analyzer (Model-926, Cole-Palmer Inc.). The tracer test results were analyzed as follows. The linear velocity was calculated from the peak arrival time of the obtained breakthrough curves, and the longitudinal dispersion coefficient was introduced from the variance of the breakthrough curves using equation (2) (Fetter, 1992):

$$D_L = \frac{\sigma^2}{2t} \quad (2)$$

where D_L is the longitudinal dispersion coefficient [m^2/sec], t is the peak arrival time of the tracer [sec] and σ^2 is the variance of the breakthrough curve [m^2]. During the experiments, the change of SP signals were recorded using 20 sintered Ag/AgCl electrodes connected with a multimeter (Model-M2700, Keithly Inc.). The multimeter was connected with the computer to collect electrical signals automatically. Fig. 4 shows the channel numbers of each electrode

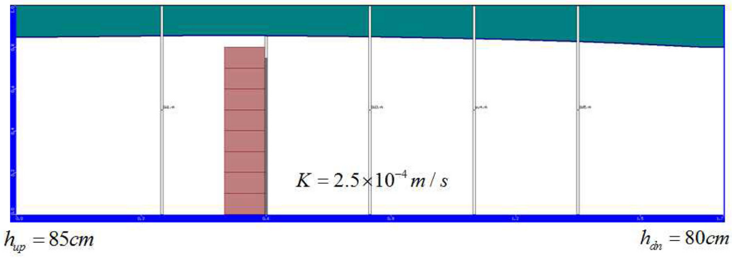

(a) Simulated water table with the injection rate of 0.005 L/sec

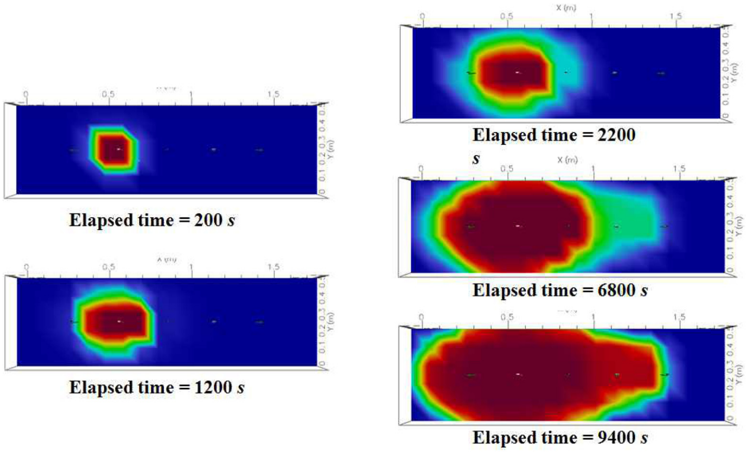

(b) Simulated tracer plume with the injection rate of 0.005 L/sec

Fig. 5. Numerical simulation results of the tracer test design.

installed in the sandbox. Note that we considered another electrode as a reference which was located beside the sandbox.

3. Results and Discussion

The hydraulic conductivity of the sandbox was estimated from the groundwater flow tests with various hydraulic head differences between upstream and downstream reservoirs. From equation (1), the hydraulic conductivity was calculated to $2.50 \times 10^{-4} \pm 2.09 \times 10^{-5}$m/sec. Fig. 5 is the numerical simulation results of the tracer test for test design. The results show that the injection rate of 0.005 L/sec into the second screened well and the head difference less than 5 cm were sufficient conditions for the dimension of our sandbox. They also indicated that sampling intervals of five minutes at first 2 hours and ten minutes for the rest of the test were enough to detect the breakthrough curves at each well.

The tracer test was conducted in two phases. In the first phase, a steady-state groundwater flow condition was established by maintaining the hydraulic heads at the upstream and downstream reservoirs and by injecting water into the injection well with the designed rate. In the second phase, we injected tracer instead of water for 5 minutes, and then injected water again to maintain water flow condition. The chloride concentrations of collected water samples during the experiment were plotted in Fig. 6. It shows that the tracer moved slowly from the injection well to other wells. The obtained breakthrough curves were similar to the normal distribution curve although the break-through curve from the third screened well (SW-3) showed double peaks. At the fourth (SW-4) and fifth (SW-5) screened wells, it was difficult to identify the breakthrough curve. Table 1 shows the analysis results of the tracer test. For SW-3, the first peak of the chloride concentration was analyzed to estimate the linear velocity and dispersion coefficient. Tracer analysis results show the variation of linear velocity and dispersion coefficient in different screened wells. From the injected well to the last screened well it shows natural

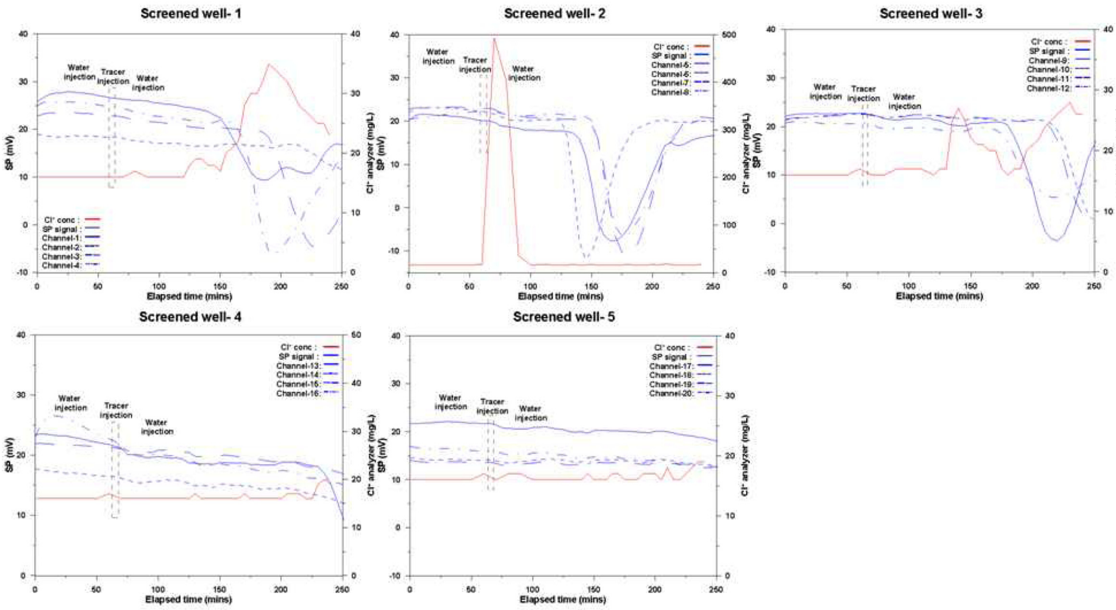

Fig. 6. Measured SP signals and Cl^- concentrations during the experiment where black dotted boxes in the graph indicates timing of tracer injection.

Table 1. Analysis results of the tracer test

Screened well	Average linear velocity, v_i (m/sec)	Hydrodynamic dispersion coefficient parallel to the direction of flow, D_L (m^2/sec)	Variance of the parallel spreading of plume, σ_L^2 (m^2)
SW-1	3.3×10^{-6}	2.8×10^{-4}	6.46
SW-3	5.5×10^{-6}	1.4×10^{-4}	4.07
SW-4	NA*	NA	NA
SW-5	NA	NA	NA

*Not Available

plume was created by the tracer solution. Here, the highest linear velocity was 5.5×10^{-6} m/sec at SW-3 and the largest dispersion coefficient was 2.8×10^{-4} m^2/sec at SW-1. However, the estimated linear velocities and dispersion coefficients were similar in the order of magnitude, respectively.

Fig. 6 also shows the distributions of SP signals data set measuring during the experiment. The black dotted boxes in the graphs indicate the duration of tracer injection. We did not found any significant change of SP signal dataset before the injection of tracer but we found signals responding to solute transport at SW-1, SW-2 and SW-3. At SW-1, the chloride concentration showed one peak at 180 to 200 minutes, and during that time SP signals also showed the reverse effect. Similarly, at other screened wells, the SP signals also changed when the chloride concentration changed. These results indicate that the SP signals are likely to be related to the solute transport.

4. Conclusions

To evaluate the feasibility of SP signals on estimation of solute transport properties of an aquifer, we conducted a tracer test with measuring SP signals. The results confirmed that the measured SP signals were produced during our experiment, and it showed significant trend or relationship between the SP and solute transport property of the sandbox during the whole period of experiment. However, we could not confirm this conclusion because there are few previous researches which provide the theoretical backgrounds of the observed phenomena in our experiments. Thus, further study to quantify the behavior of SP responding to solute transport is necessary.

Our results indicate a clue that there is a relation between SP and solute transport in an aquifer, which provides a stepping-stone for the expansion of our understanding of transport in an aquifer and reduction of the uncertainty in a tracer test.

Acknowledgement

This work was supported by the Korean Nuclear Energy R&D program of the Ministry of Science, ICT and Future Planning, Korea (NRF-2012M2A8A5007440) and the Radioactive Waste Management of the Korea Institute of Energy Technology Evaluation and Planning (KETEP) grant funded by the Ministry of Trade Industry and Energy (MOTIE), Korea (No. 2012171020001D).

References

Arora, T., Linde, N., Revil, A., and Castermant, J., 2007, Non-intrusive characterization of the redox potential of landfill leachate plumes from self-potential data, *J. Contamin. Hydrol.*, **92**, 274-292

Blake, E.W. and Clarke, G.K.C., 1999, Subglacial electrical phenomena, *J. Geophys. Res.,* **104**, 7481-7495.

Bogoslovsky, V.A. and Ogilvy, A.A., 1970, Natural potential anomalies as a quantitative index of the rate of seepage from water reservoirs, *Geophys, Prospec.,* **18**, 261-268.

Crespy, A., Revil, A., Linde, N., Byrdina, S., Jardani, A., Boleve, A., and Henry, P., 2008, Detection and localization of hydromechanical disturbances in a sandbox using the self-potential method, *J. Geophy. Res.*, **113**, B01205, doi:10.1029/2007JB005042.

Domenico, P.A. and Schwartz, F.W., 1990, *Physical and Chemical Hydrogeology*, John Wiley & Sons, New York.

Doussan, C., Jouniaux, L., and Thony, J.L., 2002, Temporal variations of SP and unsaturated water flow in loam and clay soils: a seasonal field study, *J. Hydrol.*, **267**, 173-185.

Fournier, C., 1989, Spontaneous potentials and resistivity surveys applied to hydrogeology in a volcanic area: Case history of the Chaine des Puys (Puy-de-Dome, France), *Geophys. Prospec.*, **37**, 647-668.

Fetter, C.W., 1992, *Contaminant Hydrogeology*, Department of Geology, University of Wisconsin-Oshkosh.

Jardani, A., Revil, A., Boleve, A., and Dupont, J.P., 2008, Three-dimensional inversion of self-potential data used to constrain the pattern of groundwaterflow in geothermal fields, *J. Geophys. Res.*, **113**, B09204, doi:10.1029/2007JB005302.

Jouniaux, L., Maineult, A., Naudet. V., Pessel, M., and Sailha, P., 2009, Review of self-potential methods in hydrogeophysics, *Comptes Rendus Geoscience*, **341**, 928-936.

Lorne, B., Perrier, F., and Avouac, J.P., 1999, Streaming potential measurements 1. Properties of the electrical double layer from crushed rock samples, *J. Geoph. Res.,* **104**, 17,857-17,877.

Maritinez-Pagan, P., Jardani, A., Revil, A., and Haas, A., 2010, Self-potential monitoring of a salt plume, *Geophysics*, **75**, WA17-WA25.

Mikhailov, O.V., Queen, J.H., and Toksoz, M.N., 1997, Using borehole electro seismic measurements to detect and characterize fractured (permeable)zones, *Annual Technical Report*, Massachusetts Institute of Technology, MA.

Malama, B., Revil, A., and Kuhlman, K.L., 2009a, Asemi-analytical solution for transient streaming potentials associated with confined aquifer pumping tests, *Geophys. J. Int.*, **176**, 1007-1016.

Malama, B., Kuhlman, K.L., and Revil, A., 2009b, Theory of transient streaming potentials associated with axial-symmetric flow in unconfined aquifers, *Geophys. J. Int.*, **179**, 990-1003.

Revil, A., Naudet, V., and Meunier, J.D., 2004, The hydroelectric problem of porous rocks: Inversion of the position of the water table from self-potential data, *Geophys. J. Int.*, **159**, 435-444.

Rizzo, E., Suski, B., Revil, A., Straface, S., and Troisi, S., 2004, Self-potential signals associated with pumping-tests experiments, *J. Geoph. Res.*, **109**, B10203, doi:10.1029/2004/JB003049.

Saunders, J.H., Jackson, M.D., and Pain, C.C., 2008, Fluid flow monitoring in oil fields using downhole measurements of electrokinetic potential, *Geophysics*, **73**, E165-E180.

Suski, B., Rizzo, E., and Revil, A., 2004, A sandbox experiment of self-potential signals associated with a pumping test, *Vadose Zone J.*, **3**, 1193-1199.

Titov, K., Loukhmanov, V., and Potapov, A., 2000, Monitoring of water seepage from a reservoir using resistivity and self-polarization methods: Case history of the Petergoph fountain water supply system, *First Break*, **18**, 431-435.